A MECHANISM FOR SOLID BED BREAKUP IN SINGLE-SCREW EXTRUDERS – SOLID BED SHAPE CHANGE

Gregory A. Campbell, Clarkson University/Castle Associates, Jonesport, ME
Mark A. Spalding, The Dow Chemical Company, Midland, MI

Abstract

It is well known that solid bed breakup in plasticating single-screw extruders can lead to defects in the downstream product, reduced rates, and process instabilities. After a review of the mechanism of solid bed melting an enhanced discussion will be presented regarding a new concept for solid bed break up. The literature generally attributes this breakup to pressure gradients emanating from the beginning of the metering section of the screw. In a previous paper [1] a new mechanism was proposed that was developed as a result of the physics of the melting mechanism and fluid flows associated with screw rotation physics. During the discussion after the presentation of this new mechanism at ANTEC 2013, questions were raised as to the assumptions made regarding the shape change of the solid bed during melting which the authors proposed was a result of the flow that occurs as a result of the new mechanism. In this paper more data will be presented that will help define this new concept.

Introduction

Solid bed breakup is a process that occurs in almost all plasticating single-screw extruders, and in most cases the process is undesirable since it can lead to solid polymer fragments in the extrudate, process instabilities due to solids plugging mixers, and thermal gradients [2]. Solid fragments in the extrudate will almost always cause defects in the finished product. For example, a lab extruder was operated with a mixture of 100 parts of white tinted acrylonitile-butadiene-styrene (ABS) terpolymer pellets with 1 part of black tinted ABS pellets. If the extruder operates properly without solid bed breakup, the extrudates are tinted black and are relatively uniform in color, as indicated by the cross sections shown in Figure 1 at screw speeds less than about 70 rpm. At higher screw speeds, the solid bed broke up and caused solid polymer fragments to flow downstream and into the extrudate, as indicated by the white tinted fragments at screw speeds greater than 80 rpm.

Solid bed breakup can be observed by performing a Maddock solidification experiment [3], as indicated by the photographs in Figure 2. Here the black tinted areas show regions in the screw channels that were molten at the moment of stopping screw rotation and solidifying the resin. Areas that were tinted white show regions that contain resin in the solid form. Solid bed breakup is evident in these cross sectional photographs since there are regions were the molten resin is essentially across the entire channel and solids are evident in downstream cross sections. These types of views are typical in almost all published Maddock solidification experiments.

Figure 1. Cross-sectional views of extrudate samples at a letdown ratio of 100 to 1 of a white pigmented ABS resin with a black color concentrate for a melting-mixing experiment.

Literature references discuss solid bed breakup as a phenomenon where strong forces due to pressure gradients breakup the low strength solid bed [4,5]. The source of the pressure gradients, however, is not evident and in general the pressure is higher at the end of the bed so this would logically tend to push the particles back into the bed. Zhu et al. constructed an extruder with glass inserts in the barrel for viewing the internal processes during extrusion [6] and injection molding [7]. Their observations indicated that solid bed breakup was more likely to occur at high screw speeds. For injection molding plasticators, bed breakup is more likely to occur for long injection strokes, high discharge pressure (back pressure), and long dwell times [7]. They observed small cracks that occurred across the solid bed and perpendicular to the flights in the later stages of the melting process. These cracks would then increase in width as they were filled with molten polymer. Their observations are consistent with previous researchers. The mechanism for the crack formation was not reported.

The current melting and conveying mechanisms using barrel rotation physics do not provide an explanation for solid bed breakup. Screw rotation physics, however, provides a melting mechanism and a flow mechanism that explains the solid bed breakup process in single-screw extruders.

Melting Mechanism Literature

The key to understanding solid bed breakup is the comprehension of the melting mechanism that occurs in the extruder using the actual boundary conditions for screw rotation physics. Therefore this relatively new melting mechanism will be outlined and reviewed in this section.

Recently the Polymer Processing Research group at Clarkson University reexamined the melting data published in Tadmor and Klein [4] and found that in essentially all cases the material in a conventional screw transition section disappeared in the height direction before the width direction, as shown in the reanalysis of the data in Figure 3. This was in direct contrast from the melting theory developed by Maddock [3] and the model developed by Tadmor and Klein [4]. The Tadmor and Klein model had the solid bed disappearing in the width direction only. Lindt and his research group investigated and reported a body of work trying to set up a series of complete mathematical models for the melting process. Lindt [11] developed a model by considering the solid bed in the center of the cross-section in 1976 using barrel rotation theory. Lindt focused his later work on the five-zone melting model [12-15]. Lindt, Elbirli, Gottgatreu, and Baba [12] set up a model by considering all situations that previous people considered separately. Lindt and Elbirli [13] considered the cross section circulation in the model in 1985 where the screw was still considered to be stationary. Also in 1985, Lindt claimed that "the development of the melting theory based on the Maddock mechanism has been virtually completed" [14].

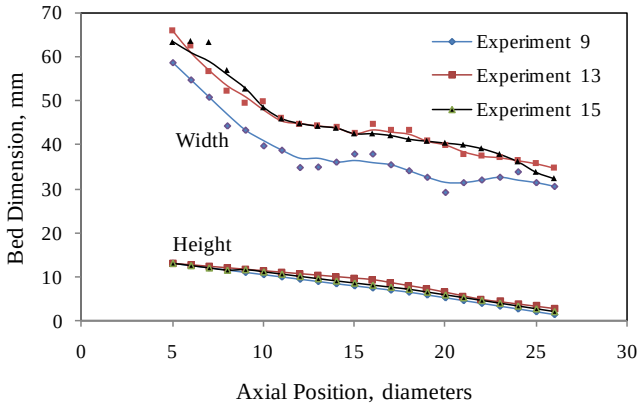

Figure 3. Reevaluation of the melting data from Tadmor and Klein for PE resins [4] as analyzed by Tang [8] and Campbell et al. [9,10].

A new melting mechanism was developed using screw rotation physics that is diagrammatically portrayed in Figure 4. The rotation of the screw creates a velocity gradient at the barrel-solid bed interface and the combination of the heat flux from the barrel and the dissipation in Film C cause the solid to melt in the negative *y* direction. The motion of the screw under the bed contributed to the energy dissipation in Film D, causing the bed to melt in the positive *y* direction. The same mechanisms occur in Zones E and B to melt the solid bed in the *x* directions. A major difference in this mechanism compared to the historic literature analysis is that the bed does not reorganize.

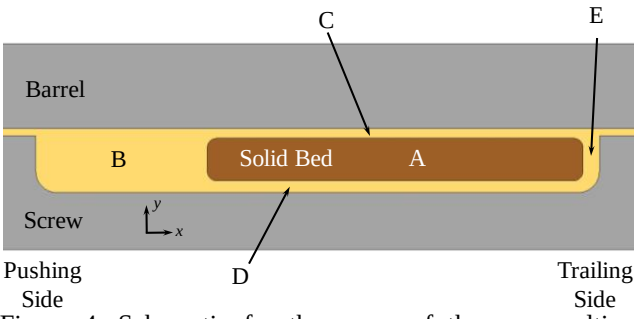

Figure 4. Schematic for the zones of the new melting concept: Zone B is the melt pool, Zone C is the melt film located between the solid bed and the barrel wall, Zone D is the melt film between the solid bed and the screw root, and Zone E is the melt film between the solid bed and the trailing flight. The cream color represents molten resin.

The Tadmor and Klein model [4] allows melting only in the Zone C film located between the solid bed and the barrel wall, as shown in Figure 4. The material melted is then dragged by the motion of the barrel and collected in the melt pool of Zone B. As melting progresses, the melt pool increases in width and the solid bed decreases in width. The solid bed is assumed to reorganize such that it covers the full depth of the channel. Near the end of melting, the Tadmor melting model and other literature models have the last remaining portion of the solid bed positioned at the trailing flight and across the full depth of the channel, as shown by Figure 5a. These models are all based on barrel rotation physics.

As previously mentioned, the Tadmor and Klein model forces all melting to occur in Zone C. The melting that occurs at the other zone interfaces with the solid bed is ignored because the velocity gradients and thus energy dissipations were believed to be very small. These gradients are due to the solid bed moving at a velocity V_{sz} calculated from a mass balance at the entry to the melting section and a stationary screw; i.e., barrel rotation physics.

Recently Campbell, Spalding, and Tang [16,17] have reexamined the assumptions in the literature models in order to address the reanalysis of the classical melting data discussed previously and shown in Figure 3. This concept was developed based on recognizing that the rate limiting

melting dynamics for solid bed consumption was in the channel height and not the channel width direction. Here the melting process occurs in all four of the melt films surrounding the solid bed, as shown in Figure 4. The boundary conditions were set to those for screw rotation physics.

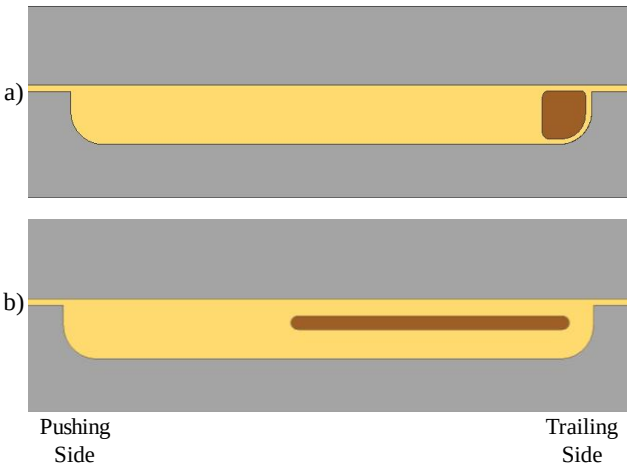

Figure 5. Schematics of the solid bed just prior to complete melting: a) the solid bed is pushed to the trailing flight with the Tadmor melting model and barrel rotation physics, and b) the solid bed is a thin plate and positioned as in the diagram (screw rotation and observation). The cream color represents molten resin.

To visualize the difference between screw rotation and barrel rotation, a simple cardboard paper towel roller can be used to model the screw core and a wood block to model the solid plug. For barrel rotation, the roller is held constant and the block is moved downstream at a velocity of V_{sz}. Here the velocity difference between the block and roller is simply V_{sz}. For screw rotation, the roller is rotated counterclockwise while the block is moved downstream with a velocity of V_{sz}. The observer will see that the core of the screw is moving in the negative z (helical) direction at a velocity of V_{cz}. The velocity difference for Zone D is as follows:

$$\Delta V = V_{sz} - V_{cz} \tag{1}$$

$$\Delta V = \frac{Q_m}{\rho_m HW} + \pi N D_c \cos\theta_c \tag{2}$$

$$\tan\theta_c = \frac{L}{\pi D_c} \tag{3}$$

where ΔV is the velocity difference between the solid bed and the root of the screw, Q_m is the mass flow rate, ρ_m is the bulk density of the solids at the start of melting, H is the channel depth at the start of melting, W is the average channel width, N is the rotation rate of the screw (rev/s), D_c is the diameter of the screw at the root (or core), θ_c is the helix angle at the screw root, and L is the lead length. The first term on the right side of Equation (2) is V_{sz} while the second term is $-V_{cz}$. A schematic of the velocity difference is provided in Figure 7. This velocity difference is considerably larger than that for barrel rotation physics. The screw rotation model presented here includes the dissipation and melting rates for all zones. The details may be found in [2].

Developing a physical model for these melt zones, leads to a description of the flow dynamics in the films that exist in the screw channel from the beginning of the melting of the solid bed through the transition section that ends at the beginning of the metering section. A schematic of a typical solid bed profile is provided in Figure 6 with the solids profile near the end of melting shown in Figure 5b for screw rotation. The fluid velocity gradient in Film C at the top of the solid bed is in the x direction which causes fluid to be deposited into Zone B. The fluid velocity in Film D between the screw root and the solid bed in Figure 4 is a more complex recirculation flow due to motion of the screw surface in the opposite direction of the solid bed. That is, the screw root motion drags fluid into the Film D gap at the end of the transition section. Some of the fluid that is dragged into Film D is thought to flow into Zone B due to a higher pressure under the solid bed than in the melt pool (Zone B). This pressure under the solid bed is a key to the mechanism for solid bed breakup.

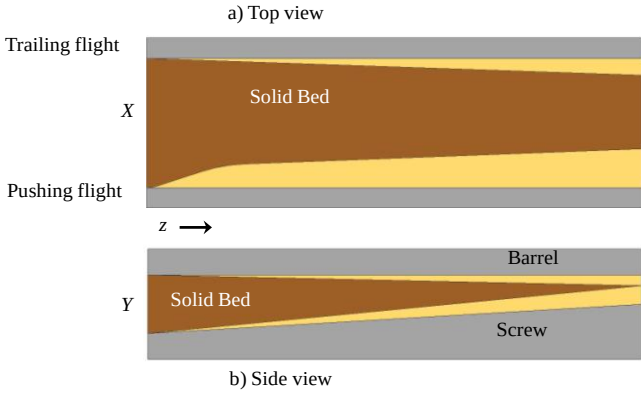

Figure 6. Qualitative shape of X and Y bed dimensions and melt film thickness for melting in a conventional transition section; a) top view, and b) side view. The cream color represents molten resin. Here X and Y are the local width and thickness of the solid bed, respectively.

For most extrusion processes, the solid bed can breakup near the completion of melting, that is in the transition as it approaches the metering section. At this point in the melting process the bed is relatively thin and

its cohesive strength is low. The strength of the bed is low at this location since the solid bed temperature is approaching the melting temperature or devitrification temperature and thus the material modulus is low. Because the bed is thin in the *y* direction there is little stability. Evidence of solid bed breakup is apparent in photographs of Figure 2. Moreover, solid bed breakup is evident in almost all reported Maddock solidification experiments for a conventional melting screw. The initiation of the breakup may be the result of the physics discussed previously from references [6,7].

The Mechanism for Solid Bed Breakup

As will be presented next, two processes are required for solid bed breakup. These processes include the melting mechanism presented above for screw rotation physics and a flow mechanism for transporting molten resin between the solid bed and the screw root.

It is obvious that the strength of the solid bed would be low near the end of melting since the bed is very thin and its temperature is approaching the melting or devitrification temperature. Based on the historical melting models using barrel rotation physics, the pressure gradients postulated for breaking the bed are difficult to produce. In general, the pressure gradient in the transition section is positive such that one might speculate that this would stabilize the bed by pushing the solids back toward the thicker and more stable portion of the bed. However, screw rotation theory leads to an alternative mechanism to those based on barrel rotation theory. Screw rotation theory is presented in great detail in [2,18-22] for the metering section. For screw rotation analysis, the barrel has zero velocity and the solid bed is moving in the positive *z* direction at a velocity of V_{sz}. The screw has a velocity of $-V_c$ and a component in the z direction of $-V_{cz}$. Here, the backward motion of the screw ($|-V_{cz}|$ or V_{cz}) is larger than V_{sz}, causing a negative pressure gradient ($\partial P/\partial z$) in Film D between the solid bed and the screw root.

There has not been an extensive technical discussion as to why the solid bed always is in close proximity to the barrel. It is thought that centrifugal force is not the primary mechanism because this phenomenon is prevalent even at very low screw rotation speeds. The locally higher pressure resulting from the rotation of the screw under the solid bed in Film D of Figure 7 is postulated to force the solid bed up against the barrel surface. This would explain the consistent observation that the solid bed is always near the barrel surface with only a thin film of fluid between the barrel and the solid bed that results from melting at the barrel-solid interface. There can be a substantial thickness of melt in Zone D. The pressure in Film C has been experimentally measured by many researchers. The local pressure in Film C is always less than the pressure in the melt pool. With the local pressure in Film C being less than that in the melt pool and with the pressure in Film D higher than the melt pool, it follows that the difference in the pressures create a force that pushes the solid bed against the barrel wall.

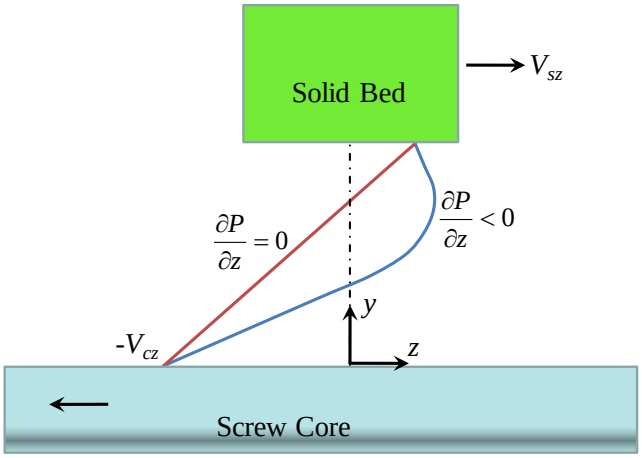

Figure 7. Schematic of the V_z velocity in the Film D between the screw core and the solid bed. The red and blue velocity lines are for pressure gradients that are zero and negative, respectively. The dotted vertical line is for $V_z = 0$.

The existence of a fluid flow back toward the solid feeding section is postulated as seen in Figure 7. For a typical melting system the pressure under the bed was calculated and is presented in Figure 8 if there were no leakage flow from Film D to the melt pool. One observes that the predicted pressure at the beginning of the melting is extremely high and well above that which is measured. The authors than went to the literature to determine if there is any evidence during the melting process where there may be flow from under the bed into the melt pool. Two sets of melting dynamics copied from Tadmor are presented in Figures 9 and 10.

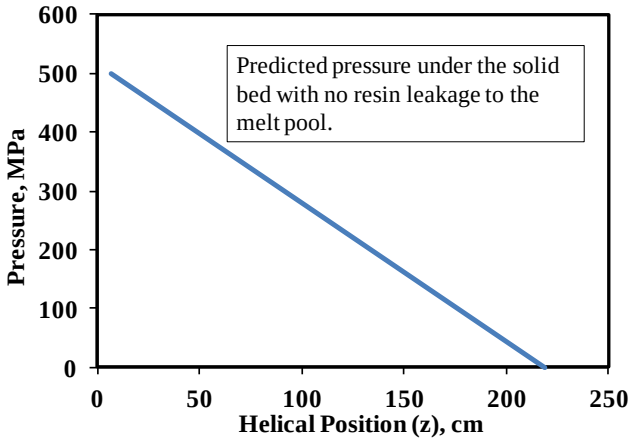

Figure 8. Predicted pressure profile under the solid bed with no resin leakage to the melt pool.

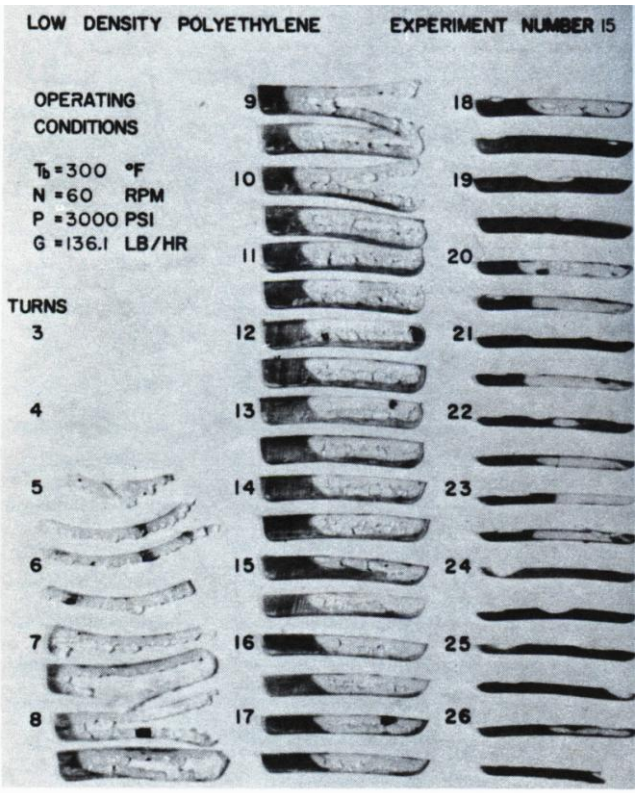

Figure 9. Melting profiles for LDPE resin from Tadmor and Klein Figure 5.16 [4].

One observes in Figure 9 that that the solid bed profile from section 7 to section 9 in contact with the melt pool is essentially a vertical surface for a low density polyethylene (LDPE) resin. However by section 17 the front of the profile shows that the bottom of the front of the profile has melted faster than the top, creating a curved interface and changing the shape of the bed.

The same general observations are made regarding this melting sequence for a polypropylene (PP) resin as shown in Figure 10.

The locally high pressure underneath the solid bed and the positive $\partial P/\partial x$ in Film D causes some flow of resin from Film D to the melt pool. Thus, for a local Δz increment for Film D, there is material entering the element from the melting process and from the drag motion of the screw core, and there is material leaving the increment from the motion of the screw core and from the flow of material into the melt pool due to a positive $\partial P/\partial x$. These complex flows are consistent with observations from Maddock solidification experiments. This flow is shown in detail for the Maddock solidification experiment shown in Figure 11.

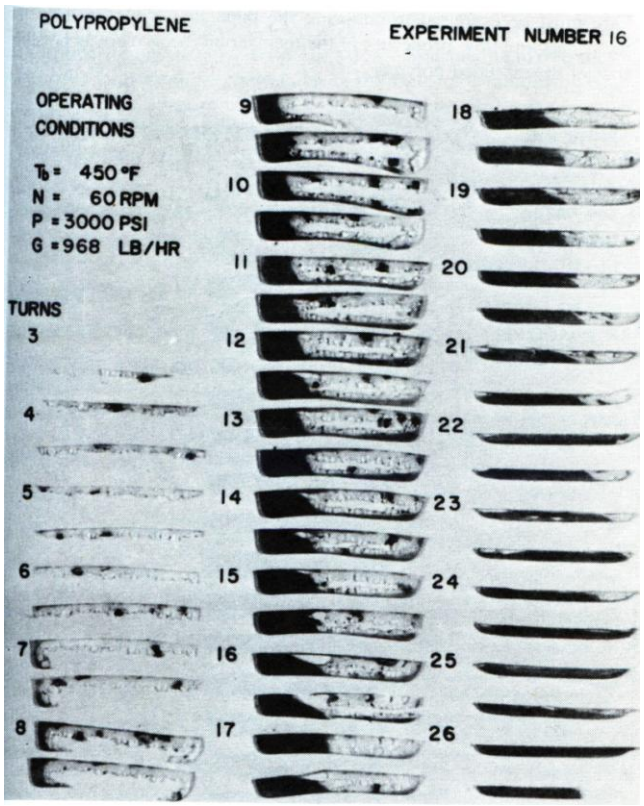

Figure 10. Melting of PP resin from Tadmor and Klein Figure 5.3 [4].

The flow from the film between the solid bed and the screw root (Film D) can be observed in most Maddock solidification experiments, as shown in Figure 11. The section in this photograph was for a location early in the melting process where the strength of the solid bed is high and can withstand the pressure gradient created by the flow induced by the backwards motion of the screw.

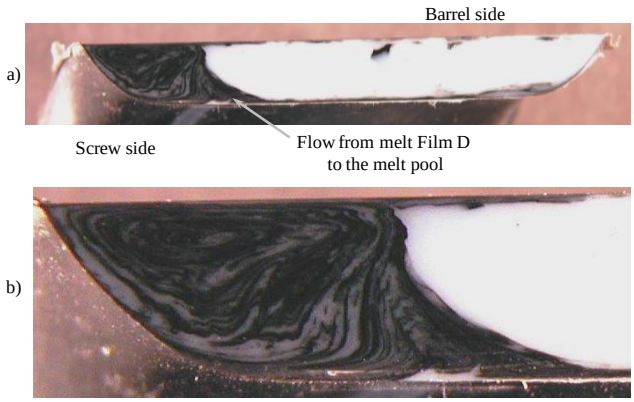

Figure 11 Photograph of resin solidified in the transition section after a Maddock solidification experiment for an ABS resin: a) the arrow is pointing at the flow lines created by the flow of material from Film D out to the melt pool, and b) an enlargement of the flow area.

The high strength of the bed prevents the bed from breaking up. Flow lines due to poor mixing of the colorant into the white resin show the flow from Film D into the melt pool (Figure 11). The flow is substantial as it is pushing and deforming the recirculating flow of the pool away from the solid bed. The fluid flowing from under the bed would be relatively hot due to shear heating as it flows under the bed. This is postulated as the cause of the more rapid melting at the base of the solid bed and causing the shape change of the solid bed at this edge. These flow patterns can be observed in Figure 2 as well with careful observation, and the observed flow pattern is not consistent with a barrel rotation model.

The qualitative expected velocities and pressure gradient are shown in Figure 7. That is, the backwards motion of the screw is dragging molten polymer backwards at the screw root and generating a significant level of pressure in Film D. When the strength of the solid bed is relatively high, the high pressure in Film D causes material to flow out to the melt pool B. If the strength of the solid bed is relatively low, then the bed will form a small crack due to the fluid flow induced stresses at the bottom interface of the solid bed, and then the crack will fill with fluid as observed by Zhu et al. [6,7]. Since the screw core develops predominately recirculating flow under the bed, the fluid would be expected to also flow under the solid bed toward the metering section (see blue line in Figure 7). This recirculating flow would cause a shear stress on the bottom of the solid bed. The upstream velocity in conjunction with the bed low cohesive energy and cracks would tend to cause fragments to break off of the bed. The surface shear stress from the recirculating fluid would thus drag the solid bed fragments away from the solid bed and into the metering section. The solid bed breakup process is qualitatively described in Figure 12.

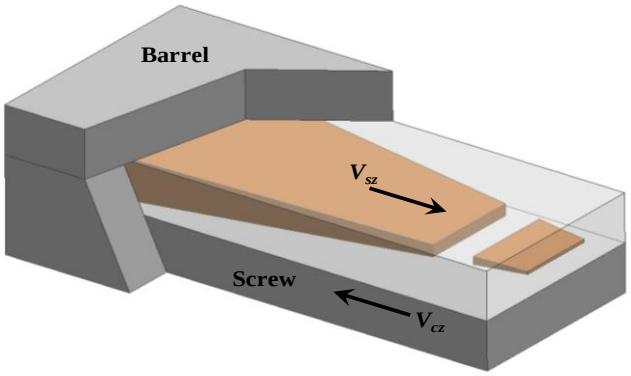

Figure 12. Schematic for solid bed breakup.

Figure 12 qualitatively describes the solid bed breakup process. For this process, the solid is moving in the V_{sz} direction. The motion of the screw drags fluid into Film D between the screw root and solid bed, creating a relatively high pressure in the film. When the strength of the solid bed is high, the high pressure induces flow out of the film into the melt pool. The flow out of Film D into the melt pool is observed in Figure 11. When the strength of the solid bed becomes low near the end of the melting process, the pressure produces a crack as shown in Figure 12, and then the crack fills with fluid as observed by Zhu et al. [6,7].

The predicted pressure under the bed with leakage flow from Film D to the melt pool is presented in Figure 13. The very high pressure as the bed approaches the 0 distance is of course not completely accurate since the liquid under the bed approaches 0 thickness at this point and there is likely a static volume where there is little or no flow.

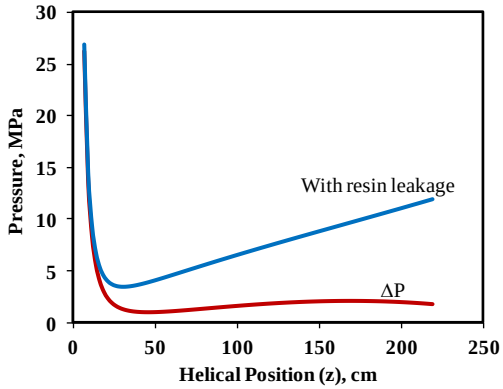

Figure 13. Predicted pressure under the solid bed.

The predicted pressure change between Film D and the melt pool, ΔP (the red line of Figure 13), decreases quickly leading to a predicted pressure profile which will provide leakage flow into the melt pool.

Discussion

The melting model based on screw rotation physics and the flow due to the negative V_{cz} velocity provides the mechanism for solid bed breakup. This paper provides more detail than originally presented in 2013 [1] on the mechanism of solid bed breakup. Barrel rotation physics and models have been unable to explain adequately solid bed breakup. The mechanism provided here is consistent with flows observed during Maddock solidification experiments and the observations by Zhu et al. [6,7].

The flow of resin from Film D to the melt pool causes some of the solid bed to melt at the interface near Film D. This melting is very obvious from the photos provided by Tadmor and Klein [4]. The melting is obvious due to the extremely small flight radii on the screws used in their experiments. Thus as melting progresses, the solid bed

edge adjacent to the melt pool changes shape as melting occurs faster at the edge near the root relative to that near the barrel surface. That is, the edge changed shape from a vertical surface to a curved surface. Since the flight radii for the screws used for the experiments in Figure 2 were considerably larger, this melting at the corner of the bed is not obvious.

The recirculating flow in the melt pool and the flow entering the pool from Film D create a region at the screw root where the flows are likely very low or form eddies. This low flow region where the recirculating and entering flow merge is shown in Figure 14. For most extrusion processes, this low flow region is not a problem and likely very difficult to detect. For thermally sensitive materials such as polyvinylidene chloride (PVDC) resin, the long residence time of the region can cause a ribbon of degraded material to form on the root of the screw where the flows merge. This ribbon typically starts when the melt pool first forms and ends when the melting process is about 70% complete. A photograph of this type of degradation is shown in Figure 15. Processing changes can mitigate this type of degradation [23].

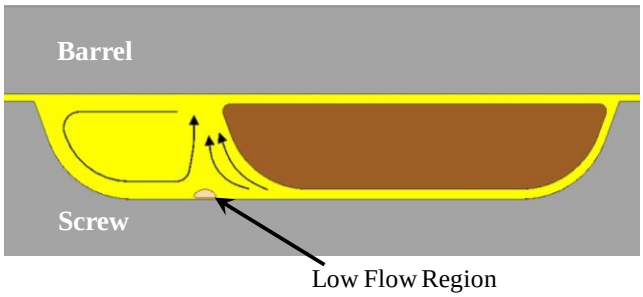

Figure 14. Schematic showing the recirculating flow in the melt pool and the flow entering the melt pool from Film D. A low flow region exists where the flow streams merge.

The degradation ribbon at the merge of the flows occurs because of the low flow region created between cross channel flow of material from Zone D and the recirculation flow in the melt pool. As shown by Figure 11, this flow from Zone D is relatively large. As previously stated, the flow occurs because of pressure induced flow and the dragging of fresh material under the solid bed by the backwards motion of the screw root. This process is consistent with the physics presented for screw rotation. The flow fields developed for a barrel rotation system would not create the low flow region such as shown in Figure 15.

For processes with relatively low compression rates such that the air entrained between the pellets is not readily pushed back out the hopper, solid bed breakup will eliminate a pathway for the air back to the hopper. In this case the entrained air will discharge with the extrudate and often create defects in the product.

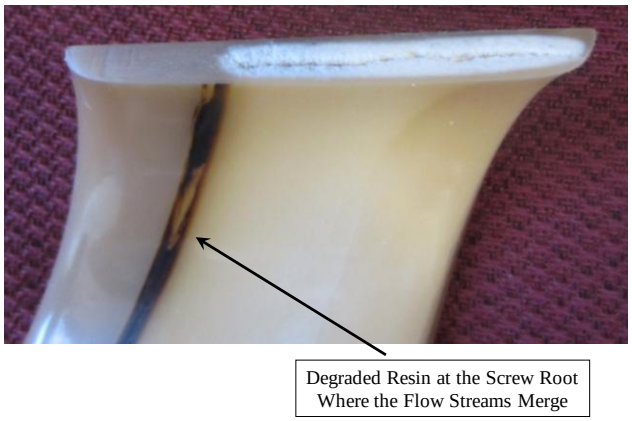

Figure 15. Photograph of a segment from a Maddock solidification experiment for a PVDC resin extrusion. The dark band is degraded resin due to a long residence time at the location.

Solid bed breakup can be mitigated using screw design and process conditions for a conventional screw design. For example, the largest single contributor to bed breakup is high screw speeds. For a particular screw, the extrudates were relatively free of solid polymer fragments at low screw speeds. But at screw speeds above about 75 rpm, solid bed breakup is occurring and high levels of solids are discharged with the extrudates. Although not desirable for a commercial process, decreasing the rate of the line is often a short term fix to eliminating solids in the discharge. Placing a finer screen in the screen pack is also an acceptable short term remedy. The best long term fix is to add an acceptable dispersive mixer to the screw or to install a high-performance screw.

Several high-performance screws actually take advantage of solid bed breakup by using the small solid fragments as a cooling method for the extrudate. For these designs, the solid polymer fragments are reduced in size using dispersive type dams. The small fragments are then melted primarily by heat conduction from the hot molten resin to the cooler solid fragments, decreasing the temperature of the molten stream. Common commercially available high-performance screws that employ this technology include Wave screws [24,25], Energy Transfer screws [26,27], Fusion screws [28], and DM2 screws [29].

Summary

The process of solid bed breakup is described and demonstrated using photographs from Maddock solidification experiments. A new theoretical hypothesis is

developed based on screw rotation theory that proposes that the bed breakup is due to the melting process and the backward flow of material under the solid bed, creating a high pressure in this gap. If this pressure is high enough to break the solid bed, solid bed breakup will occur. Flow of material from under the solid bed to the melt pool has the ability to change the shape of the edge of the solid bed that is in contact with the melt pool.

Acknowledgements

The authors are grateful to many colleagues and students that worked to develop these techniques.

References

1. G.A. Campbell and M.A. Spalding, *SPE ANTEC Tech. Papers*, **59**, 1087 (2013).
2. G.A. Campbell and M.A. Spalding, "Analyzing and Troubleshooting Single-Screw Extruders," Hanser Publications, Munich, 2013.
3. B.H. Maddock, *SPE J*., **15**, 383 (1959).
4. Z. Tadmor and I. Klein, "Engineering Principles of Plasticating Extrusion," Van Nostrand Reinhold Company, New York, 1970.
5. C.I. Chung, "Extrusion of Polymers, Theory and Practice," second edition, Hanser Publications, Munich, 2011.
6. F. Zhu, A.C.-Y. Wong, R. Liu, and T. Liu, *Plastics, Rubber and Composites Processing and Applications*, **26**, 8, 343 (1997).
7. Z. Jin, F. Gao, and F. Zhu, *Polym. Eng. Sci.*, **44**, 1313 (2004).
8. Z. Tang, MS Thesis, Clarkson University, Potsdam, NY, Chemical Engineering Department (1999).
9. G.A. Campbell, Z. Tang, C. Wang, and M. Bullwinkel, *SPE ANTEC Tech. Papers*, **49**, 213 (2003).
10. G.A. Campbell and Z. Tang, *SPE ANTEC Tech. Papers*, **50**, 162 (2004).
11. J.T. Lindt, *Polym. Eng. Sci*., **16**, 284 (1976).
12. B. Elbirli, J.T. Lindt, S.R. Gottgetreu, and S.M. Baba, *Polym. Eng. Sci*., **24**, 988 (1984).
13. J.T. Lindt and B. Elbirli, *Polym. Eng. Sci.*, **25**, 412 (1985).
14. J.T. Lindt, *Polym. Eng. Sci.*, **25**, 585 (1985).
15. J.T. Lindt, *Polym. Eng. Sci.*, **21**, 1162 (1981).
16. G.A. Campbell, M.A. Spalding, and Z. Tang, *SPE ANTEC Tech. Papers*, **55**, 147 (2009).
17. G.A. Campbell and M.A. Spalding, *SPE ANTEC Tech. Papers*, **56**, 418 (2010).
18. G.A. Campbell, P.A. Sweeney, and J.N. Felton, *Polym. Eng. Sci.*, **32**, 1765 (1992).
19. G.A. Campbell, P.A. Sweeney, and J.N. Felton, *Intern. Polym. Proc.*, **7**, 320 (1992).
20. G.A. Campbell, P.A. Sweeney, N. Dontula, and C. Wang, *Intern. Polym. Proc.*, **11**, 199 (1996).
21. G.A. Campbell, H. Cheng, C. Wang, M. Bullwinkel, and M.A. te-Riele, *SPE-ANTEC Tech. Papers*, **47,** 152 (2001).
22. G.A. Campbell, C. Wang, H. Cheng, M. Bullwinkel, M.A. te-Riele, *Intern. Polym. Proc.*, **16**, 323 (2001).
23. S.R. Jenkins, J.R. Powers, K.S. Hyun, and J.A. Naumovitz, *J. Plast. Film & Sheet*, **6**, 90 (1990).
24. G.A. Kruder, US Patent 4,173,417 (1979).
25. G.A. Kruder and W.N. Calland, *SPE ANTEC Tech. Papers*, **36**, 74 (1990).
26. C.I. Chung and R.A. Barr, U.S. Patent 4,405,239 (1983).
27. C.I. Chung and R.A. Barr, *SPE ANTEC Tech. Papers*, **29**, 168 (1983).
28. T.W. Womer, E.J. Buck, and B.J. Hudak Jr., US Patent 6,672,753 (2004).
29. M.A. Spalding, J.A. Kuhman, D. Larson, J. Kuhman, and H.L. Prettyman, *SPE ANTEC Tech. Papers*, **50**, 599 (2004).

a) $C = 2.0$, $R = 0.00190$, 61 kg/h

b) $C = 2.4$, $R = 0.00266$, 60 kg/h

c) $C = 2.8$, $R = 0.00342$, 60 kg/h

c) $C = 3.2$, $R = 0.00418$, 57 kg/h

Figure 2. Melting profiles for a 63.5 mm diameter extruder running an ABS resin at 60 rpm for screws with a 3.18 mm deep metering channel, 6 diameters of feed section, 8 diameters of transition, and 7 diameters of metering section: a) compression ratio of 2.0, b) compression ratio of 2.4, c) compression ratio of 2.8, and d) compression ratio of 3.2. The pushing flights are on the right side of the section photographs. The void marks on c) at diameters 16 through 20 were caused by the resin shrinking slightly as it cooled. Compression ratio (C) and compression rate (R) defined in reference [2].